SIMULATION OF ENTRAPMENTS IN LCM PROCESSES

René Arbter, Paolo Ermanni

Centre of Structure Technologies
ETH Zurich, Leonhardstr. 27, 8092 Zurich, Switzerland: rarbter@ethz.ch

ABSTRACT: Entrapments in liquid composite moulding (LCM) can be simulated based on elementary physical assumptions. In this contribution, mainly the conservation of the entrapped gas mass and the ideal gas law have been taken into account. In addition an algorithm tracking the evolution of the gas entrapments during the injection has been implemented. Simulation results considering non-moving and moving gas entrapments are presented and discussed. Furthermore injection experiments in a glass-tool have been performed to validate simulation results. The detection and tracking methods implemented could be verified and turned out to be reliable. Limitations of the simulation were found for small bubbles.

KEYWORDS: Liquid Composite Moulding, gas entrapment, process simulation, gas transport.

INTRODUCTION

Dry spots resulting from gas (air) entrapments are a serious problem in LCM processes Voids on mirco and meso scale have been extensively investigated in the past in order to better understand their formation and transport mechanisms and their influence on the laminate quality.
The formation of micro voids has been studied in Ref. 1. It was found that the distribution and size of voids could be explained by mechanical gas entrapment at the flow front and by the ideal gas law. In Ref. 2 the deformation of the shape and the break up of drops moving through an array of solid cylinders was investigated.
In addition to mirco voids, macroscopic gas entrapments can occur in unstable processes. These dry spots have a dramatic influence on the mechanical properties of the concerned component.

PROCESS SIMULATION

LCM-simulations including macroscopic gas entrapments have been performed using FELyX. This is an open source finite element software for solving structural problems as well as for LCM filling problems. To consider the formation of entrapments and their evolution methods for their detection and tracking were implemented.

Modeling and simulation of gas entrapments is based on following assumptions:

- Conservation of the entrapped gas mass. Absorption and/or vaporization effects between the resin and the entrapped gas are not considered.
- The entrapped air is behaving like an ideal gas. Ideal gas law is assumed to be valid
- Injection takes place at constant temperature.
- The viscosity of the entrapped gas is negligible compared to the viscosity of the resin. Thus the pressure within the gas entrapment is constant.

DETECTION OF ENTRAPMENTS

In each time step the current entrapments have to be localized. For this purpose a recursive detection algorithm for unfilled areas has been implemented in FELyX. The detection function starts at an unfilled node, marks it and marks all neighbour nodes which are not filled either. All marked nodes belong then to this unfilled area.

Unfilled areas which are directly connected to a vent are detected at first, as they can obviously not be considered as entrapments. Therefore the detection starts at each vent node. After the detection of the vent areas, all remaining unfilled areas can be identified as entrapments.

TRACKING OF ENTRAPMENTS

To calculate the current pressure within the entrapment the mass of the entrapped gas needs to be known. Mass estimation is cumbersome because the nodes belonging to a specific entrapment may change for every time step, due to the fact that new entrapments can occur between two time steps and existing entrapments can move, join, split or even dissolve. Thus the correlation between entrapment nodes during two consecutive time steps needs to be investigated. Since the location of the nodes is difficult to evaluate with respect to the membership to a certain entrapment, particularly if entrapments are close to each other, only the membership of nodes to entrapments is evaluated.

In the following we consider five scenarios, which can occur to entrapments:

- Splitting entrapment: two (or more) entrapments of the current time step consist of a high fraction (> 75%) of nodes that already belonged to an entrapment of the previous time step.
- Joining entrapments: two (or more) entrapments of the previous time step have a high fraction of nodes that belong to an entrapment of the current time step.
- New occurring entrapment: none of the previous entrapments has a high fraction of common nodes with the new entrapment.
- Dissolving entrapment: none of the entrapments of the current time step has a high fraction of common nodes with this entrapment of the previous time step.
- Moving entrapment: this is the most frequently occuring scenario. An entrapment of the current time step has a high fraction of member nodes which have belonged to an entrapment of the previous time step. Unlike for the case of a splitting entrapment only one predecessor exists.

This tracing strategy is illustrated by the following example. Five entrapments with a specified number of nodes are shown on the left side of Figure 1. On the right side a set of five entrapments is shown for the next time step.

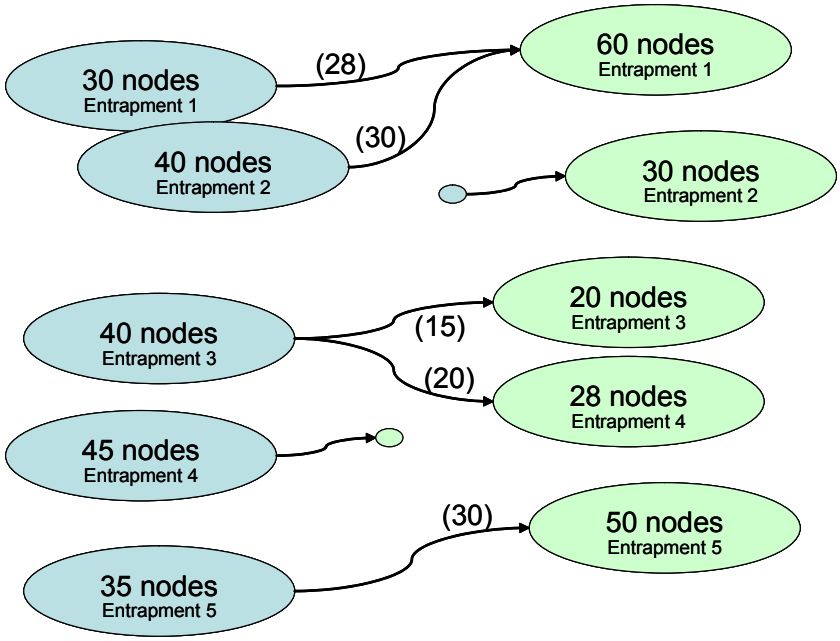

Fig 1: Entrapments and their member nodes for two successive time steps

In order to track the evolution of the entrapments, the information is bundled in two matrices as shown in Figure 2. The matrix RIN on the left side ("reappear in new") describes how many nodes of the old entrapments reappear in the new entrapments, while the matrix AIO on the right side ("appeared in old") describes how many nodes of the new entrapments already belonged to an old entrapment.

Old Entrapments \ New Entrapments	1	2	3	4	5	
1	45%	0	0	0	0	
2	50%	0	0	0	0	
3	0	0	75%	71%	0	split
4	0	0	0	0	0	
5	0	0	0	0	60%	
		new				

$$\frac{\#\text{same nodes as in previous}}{\#\text{nodes in new entrapment}}$$

RIN („Reappear in new entrapment")

Old Entrapments \ New Entrapments	1	2	3	4	5	
1	93%	0	0	0	0	
2	75%	0	0	0	0	
3	0	0	38%	50%	0	
4	0	0	0	0	0	dissolve
5	0	0	0	0	86%	
	merge					

$$\frac{\#\text{same nodes as in previous}}{\#\text{nodes in old entrapment}}$$

AIO („appeared in old entrapment")

Fig. 2: correlation matrices for entrapment tracing

Merging entrapments are characterized by columns with two or more high correlation values in the AIO-matrix, splitting entrapments by rows with two or more high correlation values in the RIN-matrix. Dissolving entrapments are characterized by rows without high correlation values in the AIO-matrix, new entrapments can be found by columns without high correlation values in the RIN- matrix. Finally, moving entrapments belong to none of the previous cases and have a high correlation either in the RIN- or in the AIO-matrix.

MOVING ENTRAPMENTS

Generally speaking, entrapments can expand or compress according to surrounding pressure changes and/or can move if they undergo a pressure gradient.

The mobility of entrapments is implemented based on elementary rules. In this context the edge of an entrapment is considered as a flow front and is simulated applying the volume of fluid algorithm [3]. Furthermore, an additional feature taking into account the the fact that no liquid can spill out of an empty control volume has been implemented.
This problem is exemplified in Figure 3. We consider an entrapment in a mesh of triangular elements (blue). The control volumes are highlighted in red. The green marked element is at the edge of the entrapment in flow direction. On the nodes 1 and 2 a pressure boundary condition is applied since both nodes belong to the entrapment. Obviously the pressure at node 3 will be lower than the pressure at nodes 1 and 2 . The resulting pressure gradient would produce a flow from node 1 and 2 to node 3, even though nodes 1 and 2 are actually empty, thus resulting in simulation errors, namely in the determination of the filling time and in the flow pattern. With respect to the simulation of the entrapment mobility, this undesired flow would also prevent node 3 from being depleted. Therefore the front edge of the entrapment would not move and entrapments would not expand when the surrounding pressure decreases.

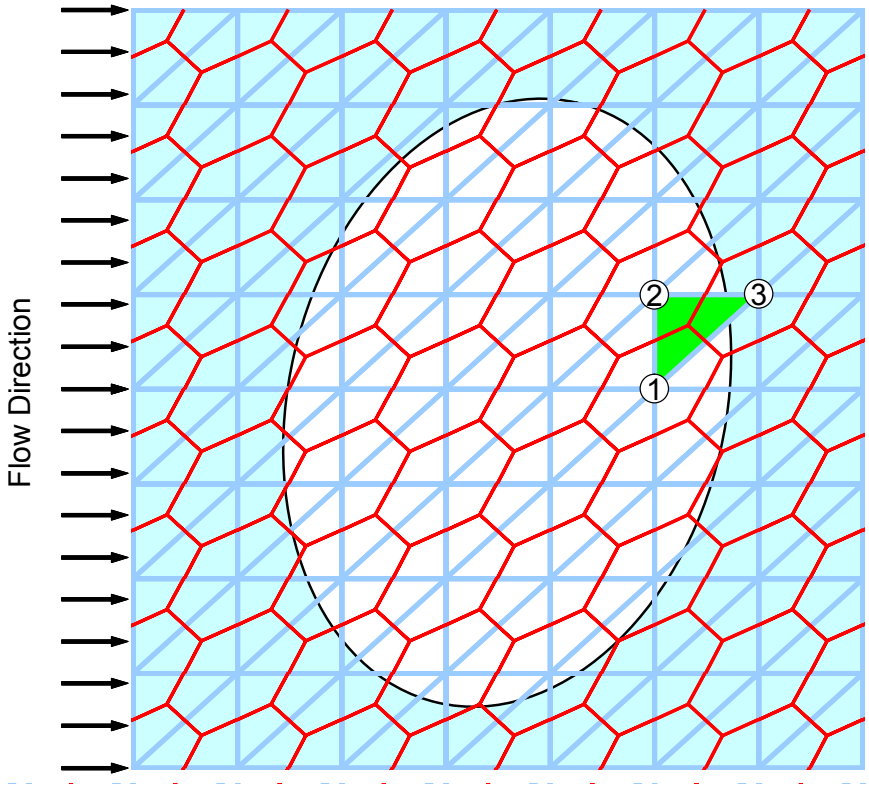

Fig 3: Control volumes and element at the front of an entrapment.

Figure 4 shows a sequence simulating the movement of a gas entrapment. The entrapment dissolves when it reaches the flow front.

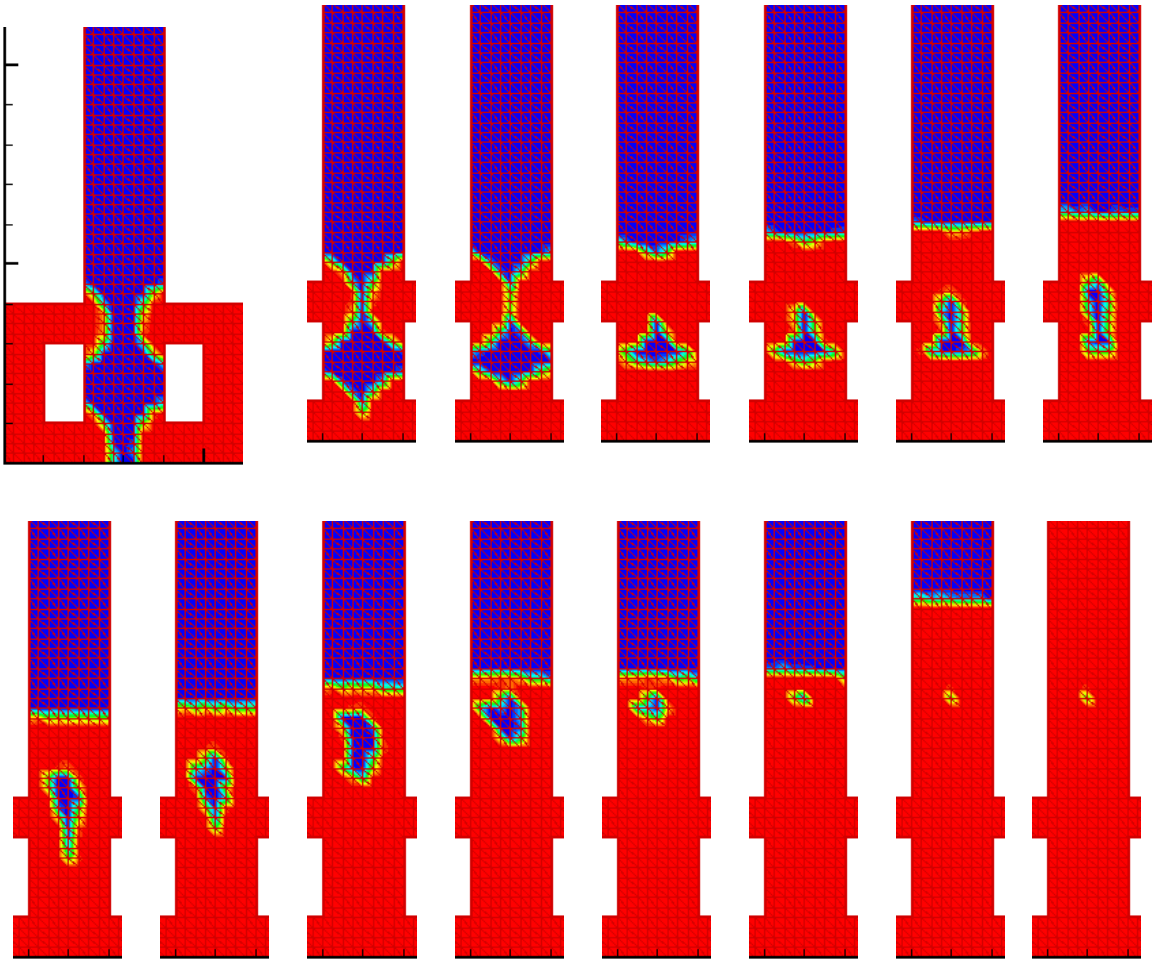

Fig. 4: Fill simulation of a moving entrapment (red regions are filled).

It can be seen that the entrapment is moving faster than the fluid. To understand this behavior a 1D flow channel is considered. Without disturbances and without entrapments there is a uniform, linear pressure distribution. This is illustrated by the resulting isobars in Figure 5 (left). If an entrapment occurs as shown on the right side of Figure 5, the pressure distribution is disturbed. High pressure gradients result on the left and on the right edge of the entrapment. (red marked areas). According to Darcy's law these high pressure gradients lead to high flow velocities on the left and on the right of the entrapment. The fast flowing resin in front of the entrapment clears the way for the entrapment and the resin behind the entrapment fills the area behind it.

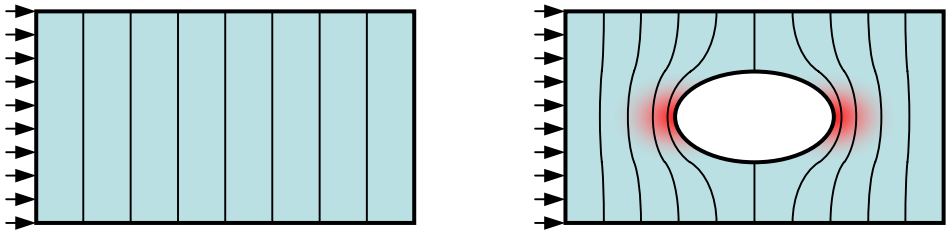

Fig. 5: pressure distribution in flow channel
without entrapment (left) and with entrapment (right)

NON-MOVING ENTRAPMENTS

Entrapments that occur in corners or that cannot move due to other reasons are compressed or expand until pressure equilibrium is reached. This mechanism is simulated using a closed flow channel without vents as shown in Figure 6). The dashed lines show the state of equilibrium for the two injection pressure values used for the simulation (50, 100….). After the pressure equilibrium between injection pressure and entrapment pressure is reached the pressure at the injection gate is reduced to $p_2 = p_1/2$. After a while, the entrapment expands again until the new pressure equilibrium is reached again. However, as highlighted in Figure 6, the straight flow front is destroyed and the resin takes the way of the least resistance. The size of the fingers depends on the mesh density, since the minimal width of a finger is determined by the width of the control volumes. In the simulation shown in Figure 6 16 elements in width were used.

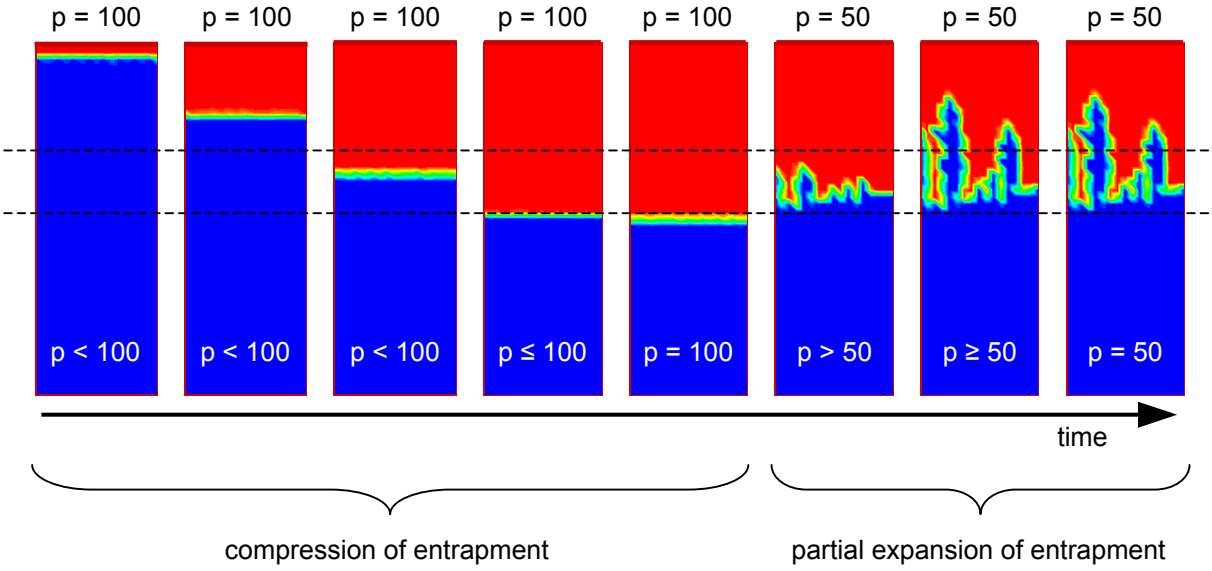

Fig 6: compressed and re-expanding entrapment

EXPERIMENTAL INVESTIGATION OF MOVING ENTRAPMENTS

The arrangement used for the simulation has been reproduced in a glass-tool in order to validate the simulation results. The sequence of pictures shown in figure 7 shows the flow pattern observed through a glass lid. A 0/90° woven fabric with 40 % fiber volume content was used.

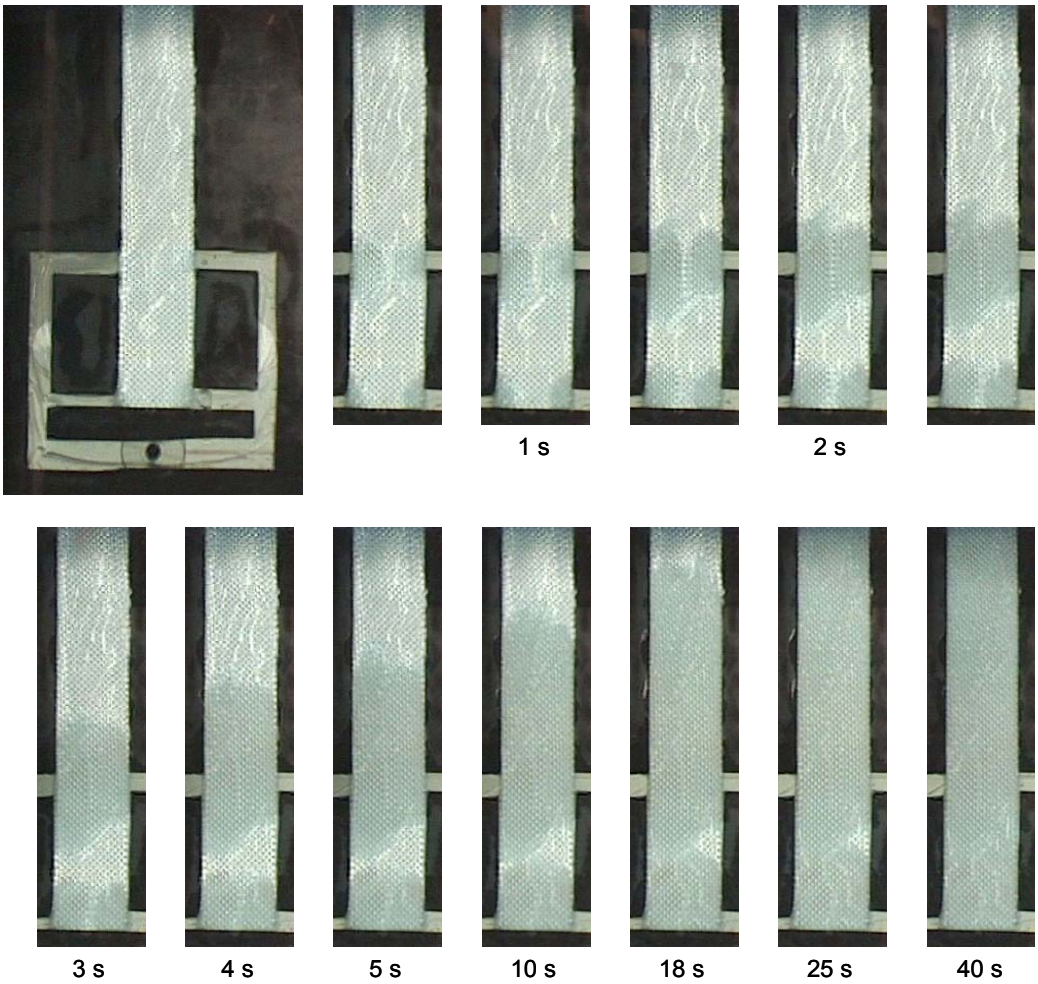

Fig. 7: entrapment evolution in a 0/90° fabric

Figure 7 shows that the entrapped air is spilled out not as a whole bubble but separated into many small bubbles. This effect could be easily seen during the injection experiments. The image in Figure 8 shows typical air bubbles traveling through the saturated areas of the laminate. These bubbles have a diameter up to 1 mm. The size might depend on the roving diameter of the used fabric.

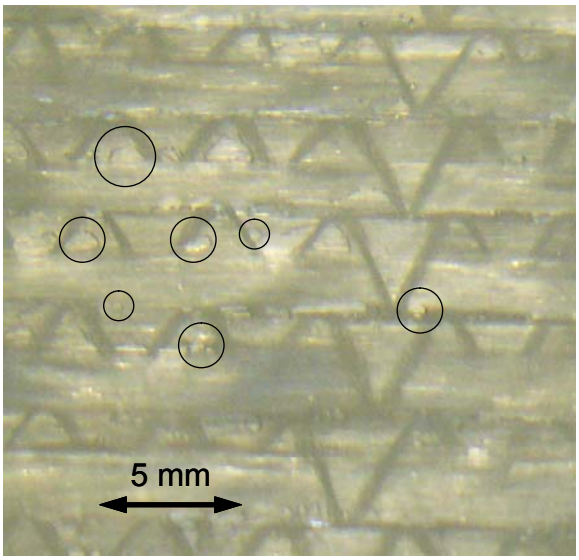

Fig. 8: small bubbles travelling through filled areas.

CONCLUSIONS

An algorithm to simulate gas entrapment mechanisms based on elementary laws has been developed and implemented in the LCM-simulation tool FELyX. The algorithm is able to detect and track gas entrapments. Results achieved so far are encouraging, showing that the algorithm is correctly simulating gas-entrapment mechanism with respect to their size and pressure..
Nevertheless the experimental program has shown, that the simplification to blur the fabric as an homogeneous porous material leads to wrong simulations of gas entrapments. As shown in Figure 7, entrapments do not vanish as one whole bubble, but as many small bubbles. Provided that entrapments appear in areas with pressure gradients toward the flow front, the resulting small gas bubbles that travel through the resin are likely to create zones with high matrix porosity. For this reason, entrapments will probably degrade the matrix quality, even if they seems to dissolve during the injection. However, in most cases entrapments don't move at all since they stay at one location, e.g. they may be trapped in a corner.

This behavior of the entrapments cannot be simulated on a macro scale using the elementary physical laws implemented in the code. The restriction of the minimal bubble size to at least one control volume makes it impossible to simulate moving entrapments realistically. Beside this, other effects like surface tension forces that are neglected in these macroscopic simulations may become important. For realistic simulations of the progression of entrapments more sophisticated entrapment models taking into account the different nature of the flow progression in and between the fibre bundles will be required.

REFERENCES

1. T. S. Lundström, B. R. Gebart, C. Z. Lundemo, "Void formation in RTM", *Journal of Reinforced Plastics and Composites,* Vol. 12 (1993).

2 K. Kang and K. Koelling, "Void transport in resin transfer molding ", *Polymer Composites,* Vol. 25(4), pp. 417-432 (2004).

3. C. W. Hirt and B. D. Nichols "Volume of Fluid (VOF) Method for the Dynamics of Free Boundries", *Journal of Computational Physics*, Vol. 39, pp. 201-225 (1981).